J. Nanostruct., 6(2): 154-164, Spring 2016
DOI: 10.7508/jns.2016.02.008

ORIGINAL RESEARCH PAPER

High Pt Loading on Polydopamine Functionalized Graphene as a High Performance Cathode Electrocatalyst for Proton Exchange Membrane Fuel Cells

Monireh Faraji[1], Hussein Gharibi[2], Masoumeh Javaheri[3]*

[1]*Chemistry Faculty, North Tehran Branch, Islamic Azad University, Tehran, Iran, P.O.Box .11155-9161*
[2]*Department of chemistry, Faculty of Science, Tarbiat Modares University, Tehran, Iran P.O.Box-335-14115*
[3]*Department of Ceramic, Material and Energy Research Center, Tehran, Iran P.O. Box: 31787-316,*

ARTICLE INFO.

Received 24/02/2016
Accepted 27/03/2016
Published online 01/04/2016

KEYWORDS
Pt nanoparticles
Oxygen reduction reaction
Graphene
Fuel cell

ABSTRACT

Morphology and size of platinum nanoparticles are a crucial factor in improving their catalytic activity and stability. Here, we firstly report the synthesis of high loading Pt nanoparticles on polydopamine reduced Graphene. The loading concentration of Pt (nanoparticles) NPs on Graphene can be adjusted in the range of 60-70%.With the insertion of polydopamine between Graphene oxide sheets, stacking of Graphene can be effectively prevented, promoting diffusion of oxygen molecules through the Graphene sheets and enhancing the oxygen reduction reaction electrocatalytic activity. Compared to commercial catalysts (i.e., state-of-the-art Pt/C catalyst) the as synthesized Pt supported polydopamine grafted reduced graphite oxide (Pt@PDA-rGO) hybrid displays very high oxygen reduction reaction catalytic activities. We propose a unique 2D profile of the polydopamine-rGO role as a barrier preventing leaching of Pt into the electrolyte. The fabricated electrodes were evaluated with electrochemical techniques for oxygen reduction reaction and the obtained results were further verified by the transmission electron microscopy micrographs on the microstructure of the integrated pt@PDA-rGO structures. It has been revealed that the electrochemical impedance spectroscopy technique can provide more explicit information than polarization curves on the performance dependence on charge-transfer and mass transport processes at different overpotential regions.

How to cite this article
Faraji M, Gharibi H, Javaheri M. High Pt Loading on Polydopamine Functionalized Graphene as a High Performance Cathode Electrocatalyst for Proton Exchange Membrane Fuel Cells. J Nanostruct, 6(2): 154-164. DOI: 10.7508/jns.2016.02.008

INTRODUCTION

Proton exchange membrane (PEM) fuel cells are environmentally friendly promising power sources for future. They exhibit great energy efficiency and high power density per volume[1]. Platinum (Pt) is known as the best electrocatalyst for PEM fuel cell gas diffusion electrodes (GDE) due to its possession of a high exchange current density for both the H_2 oxidation and O_2 reduction reactions in the fuel cell.[2] In the early developed PEM fuel cell, the Pt catalyst loading in gas diffusion electrodes was at the rate of 28 mg/cm^2 resulting in the high cost of fuel

*Corresponding author Email address: *monireh.faraji@gmail.com*

cell [3]. To minimize the Pt utilization, Pt particles were dispersed as small particles on the surface of support materials that provide a structural, conductive and durable support for the active metal particles[4]. The applying of the support material can alter the shape of the catalyst particles; enhance the activity of the catalytic sites on the metal surface and the number of active sites and impacts on electronic and geometric properties of electrocatalyst [5].

The popular support material used in PEM fuel cells is carbonaceous support materials such as Vulcan XC-72, Ketjen Black or Black Pearl 2000, due to their high electrical conductivity and high speciuc surface area. However, the main drawback of these carbon supports is oxidation at high potentials (0.207<V/NHE at 25 °C) over time. Thus, many studies have focused on alternative low-cost, high-performance and noncorrosive electrocatalyst support materials that enable faster electron transfer and high electrocatalytic activity [6,7], and these include both modiued carbonaceous and non-carbonaceous materials and these include both modiued carbonaceous and non-carbonaceous materials.

Among those carbon materials Graphene has attracted considerable interest and has become the focus of much research since its discovery in 2004. It has extraordinary properties such as high speciuc surface area (2630 m^2/g), high thermal conductivity (5000 W/m K) [8].These distinctive and intriguing features make this highly versatile carbon material promising in many potential applications such as transparent conducting films sensors, bioanalysis, and so on. Recently, as a supreme support, Graphene decorated with metal nanoparticles, metal oxide nanospheres, and polymers has been reported as catalyst materials [9-11]. Seger synthesized Pt/Graphene nano-composites sheets and examined their utilization in proton exchange membrane assembly [12]. Yoo et al. prepared a new Graphene supported elctrocatalyst for methanol oxidation in direct methanol fuel cells [10]. Guo etal synthesized three dimensional Pt-on-Pd bimetallic nanodendrites supported on Graphene to utilize as an electrocatalyst for methanol electrooxidation [13].

Van der Waals interactions cause, the as reduced Graphene nanosheets tend to form irreversible agglomerates [14,15]. Attaching some molecules or polymers onto the Graphene sheets is a usable method to prevent aggregation and keep Graphene as individual sheets [16,17]. In order to apply Graphene as support for Platinum as an electrocatalyst for PEM fuel cells reactions, physical features like surface area and electrical conductivity of Graphene should be optimized. To solve this problem, some other intermediates have to be introduced. Qu *et al.* indicate that homogeneous and ultra fine spherical Pd nanoparticles are densely in situ decorated on DNA-modified Graphene surfaces and the prepared DNA- Ge Pd hybrid shows high catalytic activity for fuel cell formic acid electro-oxidation [18]. Zhang *et al.* used poly-(diallyldimethyl-ammoniumchloride) PDDA to facilitate the in situ growth of highly dispersed Pt nanoparticles on the surface of Graphene nanosheets to form Pt/Graphene nanocomposites. They prepared well-dispersed Pt nanoparticles with small particle size on PDDA-functionalized Graphene [19].

Dopamine (DA), an environmental friendly organic chemical which consists of an repetitive catechol-amine structure of 3,4-dihydroxyl-L-phenylalanine, Ortho dihydroxyphenyl compounds, could be found in mussel's foot protein, and possess outstanding adhesive capability to various substrates [20,21]. Dopamine could be used as reducing agent with oxidation of catechol groups to the quinine form [22]. Xu *et al.* successfully employed dopamine derivatives to reduce and non-covalently functionalize Graphene oxide. Moreover, the remaining amine after oxidation of dopamine can react with epoxy group when dopamine has been used as reducing agent, which could prevent the agglomeration of Graphene into graphitic structures As a result; it is promising to utilize DA to reduce GO [20]. Dopamine can be self-polymerized to form polydopamine (PDA) in weak alkaline solution; catechol groups of the PDA ulm can produce an extremely versatile platform for further reactions. The metal ions such as Fe^{+3} and Ti^{4+} can be directly immobilized on the polydopamine. Huang *et al.* prepared novel yolk/shell Fe_3O_4 polydopamine Graphene Pt (Fe_3O_4@PDA/RGO/Pt) nano-composites synthesized using polydopamine as a moderate modifier for Graphene as well as a coupling agent for the assembly of Pt nanoparticles [23]. Tian et al. constructed bioelectrochemical sensing platform based on AuNPs/PDRGO nanocomposite. They claimed that the residue moiety of catechol in the AuNPs/PDRGO hybrid system can efficiently accelerate the electrochemical oxidation of NADH via

electron transfer [24]. Zhang et al reported the preparation of Pt NPs (~4.2 nm) which is uniformly dispersed on the PDA/RGO surface. The as-prepared composites display high electrocatalytic activity toward the reduction of H_2O_2 and O_2 [25]. Jiu et al. prepared core–shell AgNPs@PDA nanostructures and investigated high photocatalytic ability of the hybrid composites [26].

In spite of literatures described above involve the use of DA and PDA to reduce and functionalize Graphene oxide, the design of Pt nanoparticles based on PDA-functionalized.

Graphene as an electrocatalyst for oxygen reduction reaction in PEM fuel cells electrodes is relatively unexplored. The aim of this work was to design and synthesize a novel electrocatalyst support material for high loading Pt nanoparticle with polydopamine coated on the surface of Graphene. As a result, the resultant small sized Pt nanoparticles were uniformly dispersed on surface of Graphene, and its loading density could be controlled.

MATERIALS AND METHODS

GO was prepared from graphite powder (Merck) by the method of modified Hummers and Offeman [27]. In a common procedure, 50 mL of H_2SO_4 was added into a 500 mL uask containing 2 g graphite at room temperature. The uask was cooled to 0°C in an ice bath. Then 6 g potassium permanganate (KMnO4) was combined slowly to the above mixture and allowed to warm to room temperature. The suspension was stirred continuously for 2 h at 35 °C. After that, it was cooled in an ice bath, and subsequently, diluted by 350 mL of deionized water. Then H_2O_2 (30 v/v%) was added to reduce residual permanganate to soluble manganese ions, until the gas promotion stopped. Finally, the resulting suspension was ultered, washed with water, and dried at 60 °C for 24 h to take graphite oxide.

After that, the as-prepared graphite oxides were exfoliated by ultrasonication in a water bath (150 W) for more than 2 h. Finally, a homogeneous Graphene oxide aqueous dispersion (0.5 mg/mL) was obtained.

10 mg exfoliated Go,10.8 mg of H_2PtCl_6 and Hydrazine hydrate (1.00 mL,32.1mmol) added to the round bottom solution refluxed and heated in an oil bath at 120 °C under argon atmosphere for 24 h, the black product washed, filtered and dried in vacuum oven [28].

Polydopamine incorporated GO paper (PDA-GO) sheets were prepared simply. Dopamine hydrochloride (20 mg) was made in a 10 mM Tris-buffer solution (pH 8.5). 10 mL GO suspension (1 mg/mL) dispersion was then added dropwise into the above solution under magnetic stirring and the solution was sonicated for 0.5 h. After quietly stirring for about 24 h, filtration, washing and drying, PDA-GO was obtained. Afterward, 25 mg PDA-GO was sonicated in 50 ml of ethylene glycol (EG) for 20 min, followed by the addition of 10.8 mg of H_2PtCl_6 and the adjustment of pH to 8.0 by NaOH. The mixture was sonicated for 20 min for certain association of H_2PtCl_6 with PDA-GO composite, and reuuxed at 110 °C for 2 h. Finally, the solid product was ultered, rinsed and dried at 50 °C for 24 h [29]. The synthesis direction of Pt @ PDA-GO is illustrated in Fig. 1.

The micro porous layer (MPL) was prepared using the following procedure [30]: The activated carbon powder (Vulcan Xr 72) was mixed with 30wt%. PTFE water solution(isopropyl alcohol and glycerol in an ultrasonic bath for 30 min.

The resulting carbon slurry was coated onto one side of the carbon paper (TGPH-0120T) (Toray) substrate using a brushing method at 80 °C to make the MPL uniform and compact. In order to evaporate all residual glycerol, the MPL sample was heat-treated at 280 °C for 30 min then at 350 °C for 30 min to uniformly distribute PTFE throughout the MPL. In the MPL, the carbon loading was maintained 70wt%.

The method of the catalytic ink preparation was as follows: (1) addition of required amount of Pt catalyst powder and Nafion solution. The loading of Nafion in the catalyst layer was fixed at 15 wt.% and the metal loading was 0.2 mg cm^{-2} (2) addition of appropriate amount of solvent (water–isopropanol mixture (2:1 by weights) amount of solvent dependent on the amount of catalyst, ensuring the constant viscosity of the catalytic ink; (3) homogenizing the mixture using a sonicator (Misonix Model S-3000) for 20 min [31].

GDEs were prepared by applying catalytic ink onto the MPL in several layers. Brushing or spraying was employed for this purpose. The amount of deposited catalyst was detected by weighting. A Pt load of 0.2mg cm^{-2} was used throughout the study [32].

Chemical structures of GO and PDA-rGO were investigated by Fourier transform infrared Thermo Scientific. AlmegaThermo Nicolet Dispersive Raman

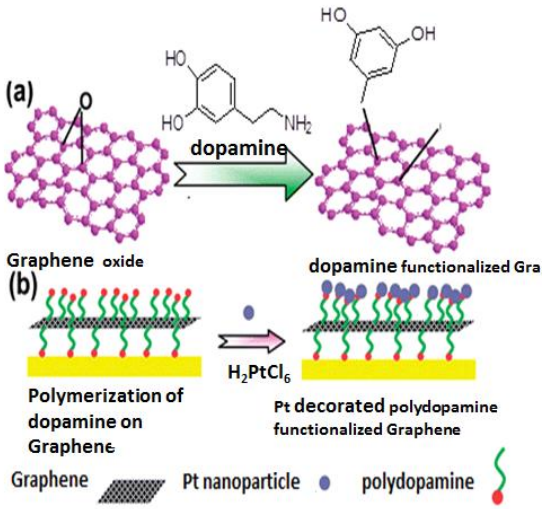

Fig. 1. (a) GO functionalization with dopamine (b) In situ polymerization of dopamine and (c)reduction of GO and in situ deposition of Pt precursor, Pt@PDA-rGO

spectrometer was used to study the structural changes in graphite, Go and Graphene with second harmonic @532 nm of Nd:YLFlaser. Raman spectra was obtained from a thin film sample which is deposited on a silica wafer at room temperature. Samples for Fourier transform infrared (FTIR) were fabricated by mixing a small amount of prepared powders with potassium bromide powder, and pressing into pellets in a die.

XRD analysis was carried out operating at 40 kV out for the Graphene and catalysts by using an XPERT MPD Philips diffractometer with a Cu X-ray source and 40 mA. The XRD patterns were obtained at a scanning rate of 1°/min with a step size in the 2θ scan of 0.02° in the range 5-100°. The Pt content in catalysts was estimated by inductively coupled plasma (ICP) analysis.

An EG&G Princeton Applied Research Model 273A instrument and frequency response detector (model 1025) were used to determine the electrochemical properties of electrodes. The performance of the GDEs (geometric exposed area 1 cm^2) in the reduction of oxygen was investigated in 0.5M H_2SO_4. All measurements were performed at 25°C in a conventional three-electrode cell, with O_2 flowing at 50 mL min^{-1}. The GDEs were mounted into a Teuon holder that contained a pyrolytic graphite disk as a current collector and has provision for feeding oxygen from the back of the electrode. A large area platinum uat electrode was used as the counter electrode. An Ag/AgCl reference electrode was placed close to the working electrode surface. A glassy carbon electrode immersed in 0.5 M H_2SO_4 was used to perform cyclic voltammetry. The electrochemical cell was connected to a potentiostat galvanostat (EG&G Model 273A) for IeV polarization measurements and, for electrochemical impedance spectroscopy. In order to perform a quantitative evaluation of resistance against the ORR, the AC impedance method was used. All experiments were performed at room temperature in a conventional three-electrode cell assembled with glassy carbon (GC) disk (0.0314 cm^2 as the working electrode).

RESULTS AND DISCUSSION

To ensure whether GO reduced by PDA, FT-IR spectra of PDA-rGO, and GO were obtained. As shown in Fig. 2 in the FT-IR spectra of GO multiple peaks were clearly observed at 1044 cm^{-1} (hydroxyl C–O stretching), 1209 cm^{-1} (epoxy C–O stretching vibration), 1615 (aromatic C=C stretching), 1715 cm^{-1} (carboxyl C=O stretching), and strong broad peak 3420 cm^{-1} (O–H stretching). In the FT-IR spectra of PDA-rGO nano-composite, the band at 3420 cm^{-1} of OH group and the band at 1715 cm^{-1} of carbonyl group disappeared, indicating that GO was totally reduced by dopamine and rGO was formed [33]. The band at 3400 cm^{-1} can be attributed to the NH group of PDA, indicating that PDA was self-polymerized and PDA-rGO nanocomposite was produced.

Fig. 3 shows XRD patterns of pristine graphite, Graphene oxide, and Pt@PDA-rGO composites. The X-ray (002) peak of the pristine graphite is observed at 2θ value of 26.4°, indicating an interlayer distance

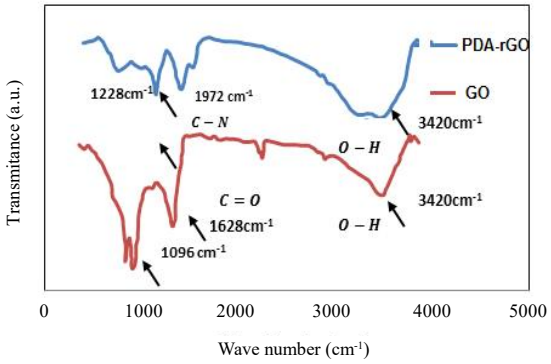

Fig. 2. FT-IR spectra of, pure GO and PDA-rGO

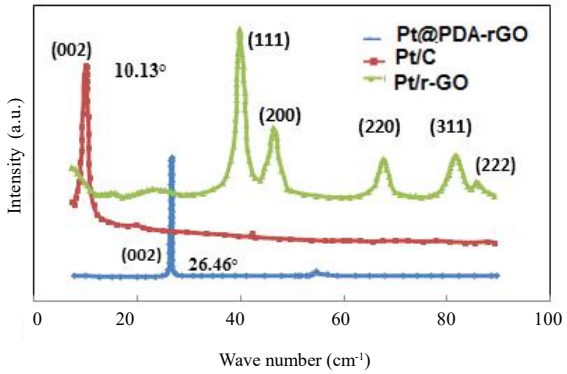

Fig. 3. XRD pattern of pristine graphite, GO, and Pt@PDA-rGO

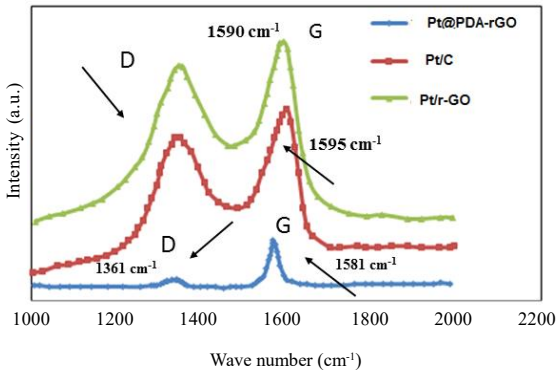

Fig. 4. Raman spectra of graphite, GO, and PDA-rGO.

of 0.35 nm. The presence of intercalated H_2O molecules and various oxide groups leads to a large interlayer space (d_{002}=7.9 Å) for the (002) peak at 2θ=10.130° for GO. PDA-rGO had higher d-spacing value (PDA-rGO = 9.7 Å) than GO (d_{GO} = 7.9 Å). Such the increased d-spacing value in PDA-rGO is due to the intercalation of PDA between the stacked GO sheet interlayers.

The Raman spectra for Graphene oxide, and after reduction with PDA, are shown in Fig. 4 the D band is ascribed to the edges, defects and disordered carbon atoms, whiles the G band corresponds to sp^2 bonded carbon atoms. G band in graphite is obviously intense (the E_2g mode of sp^2 carbon atoms) whereas D band is very weak (the symmetry A1g mode) at 1581 cm^{-1} and 1361 cm^{-1}, respectively. Compared to that of graphite, the G band of GO becomes broadened and shifts to 1595 cm^{-1} while its D band changes remarkably indicating increased disorder, which is in accordance with the result of FT-IR spectra. Meanwhile, the G bands of PDA-rGO sample move to lower wave number regions close to that of graphite, showing that the GO has been reduced to some degree after treatment with PDA. The ID/IG was increased respectively from 0.21(graphite) to 0.83 (GO) and (PDA-rGO) 1.03, owing to the fact that reduced state increases the number of aromatic, smaller-sized sp^2 domains in PDA-rGO sample.

SEM image of GO consists of crumble forming irregular separated structures, expanded and leafy structures of graphite oxide layers After reduction reaction of GO with PDA Graphene sheets made of a few Graphene layers could be clearly seen in Fig. 5(a) and (b) Consequently, the reduction procedures led to the formation of Graphene nanosheets which have highly porous and wavy structure. The composition of the Pt@PDA-rGO was determined by ICP. The Pt content is obtained about %60.

Graphene nanosheets are recognizable in the TEM image of PDA-rGO. A typical TEM image of the Pt supported on PDA-rGO is shown in Fig. 4(c) and (d). It obviously shows that high Pt loading with uniform size homogeneously decorated on the Graphene nanosheet which is in a good agreement with ICP analysis. It is due to that PDA is a mild reducing agent and an effective linker as a result; it can control the rate of reduction and regulate the morphology of Pt nanoparticles, which is crucial for obtaining small Pt nanoparticles.

The X-ray diffraction (XRD) pattern of the Pt@PDA-rGO nanocomposites in the range of 10-90° is shown in Fig 2. The (002) diffraction peak around the 2è value of 23° indicates the crystalline nature of the graphitic structure of Pt@PDA-rGO. The five characteristic diffraction peaks between 30° and 90º at Bragg angles of about 39.69°, 46.35°, 67.1°, 81.3, and 85.46° correspond to the (111), (200), (220), (311) and (222) Pt facets [32] The average particle size for the Pt@PDA-rGO catalysts is calculated from the broadening of the (220) diffraction peaks using Scherrer's equation:

$$d = \frac{0.9\lambda}{B_{2\theta}\cos\theta_{max}} \quad (1)$$

where d is the average particle size in nm, l the wavelength of the X-ray (1.5406 Å), θ the angle at the maximum of the peak, and B2è the width of the peak

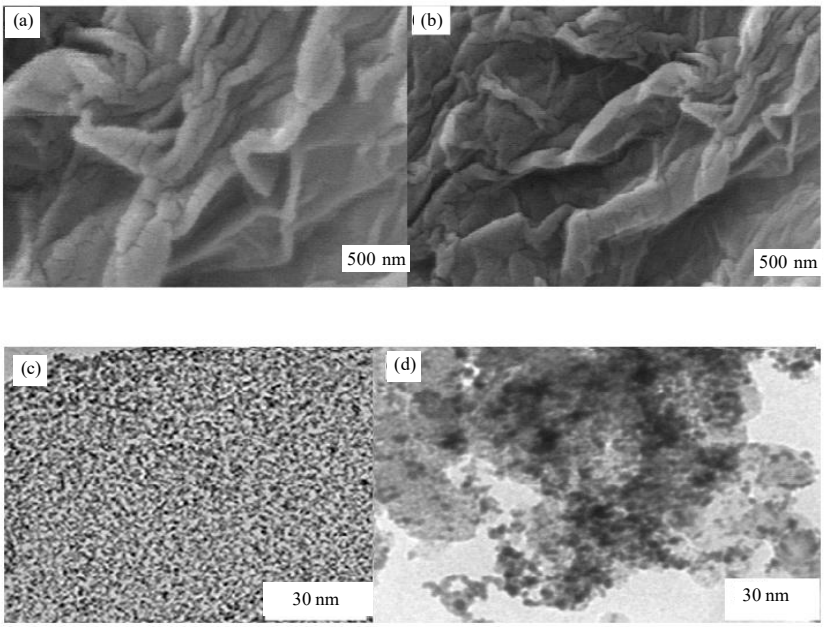

Fig. 5. (a) ,(b)SEM images of GO and PDA-rGO,TEM images of,(c) %60 Pt@PDA-rGO 100nm,(e) %60 Pt@PDA-rGO30nm

at half-height [33]. The obtained value is 3.5 nm, which is consistent with the TEM results.

Electrochemically active sites, the ECSA, in Pt@PDA-rGO which is fundamental for realization of the utility of electrocatalyst was obtained by cyclic voltammetry (CV). Hydrogen adsorption/desorption in an electrochemical phenomena is usually used to the measure ECSA. As shown in Fig. 6(a), well-defined hydrogen adsorption/desorption characteristics in the potential region of -0.2 to1.2V (vs. Ag/AgCl) are observed for the Pt@PDA-rGO (Pt loading 60 wt%) and Elctrochem (10wt%) catalysts. The columbic charge for hydrogen desorption was used to calculate the electroactive surface area (ECSA) of each catalyst. The integrated area under the adsorption peak in the CV curves represents the total charge concerning H^+adsorption, Q_H, and has been used to determine ECSA by employing the equation [34]:

$$EAS = \frac{Q_h(\mu C/cm^2)}{210(\mu C/cm^2)\times[Pt](mg/cm^2)} \quad (2)$$

The ECSA of Pt in different catalyst are shown in Table 1. Small size of Pt nanoparticles dispersed uniformly on Graphene nanosheets leads to this illustrious result. The ECSA of Pt in different catalyst are shown in Table 1. Small size of Pt nanoparticles dispersed uniformly on Graphene nanosheets leads to this illustrious result. This result reveal that the utilization of Pt in the Pt/Graphene nanocomposites is very high, which is very important for improving the practical performance of PEMs and gas phase catalytic reactions the permeabilites of oxygen in the different electrodes were determined by chronoamperometry. Chronoamperograms were obtained by holding the potential of the GDE at 1.2 V for 60 s and then stepping it to 0.3 V relative to the Ag/AgCl electrode for 10 s with oxygen flowing along the back of the electrode Fig. 5(b) plots I versus $t^{-1/2}$ for the oxygen reduction, which shows the presence of the following linear relationship for different electrodes and is given by the modified Cottrell equation [35]:

$$I(t) = \frac{nFD_b^{1/2}c_b}{(\pi t)^{1/2}} + \pi nFD_b c_b r \quad (3)$$

where A is the geometric area of the electrode, D_b the diffusion coefficient, c_b the concentration of oxygen, r the radius of the microelectrode, n the number of electron in the overall reaction of ORR, F the Faraday's constant, t the time, and π is equal to 3.14. Permeability is simply the product of $D_b c_b$ the

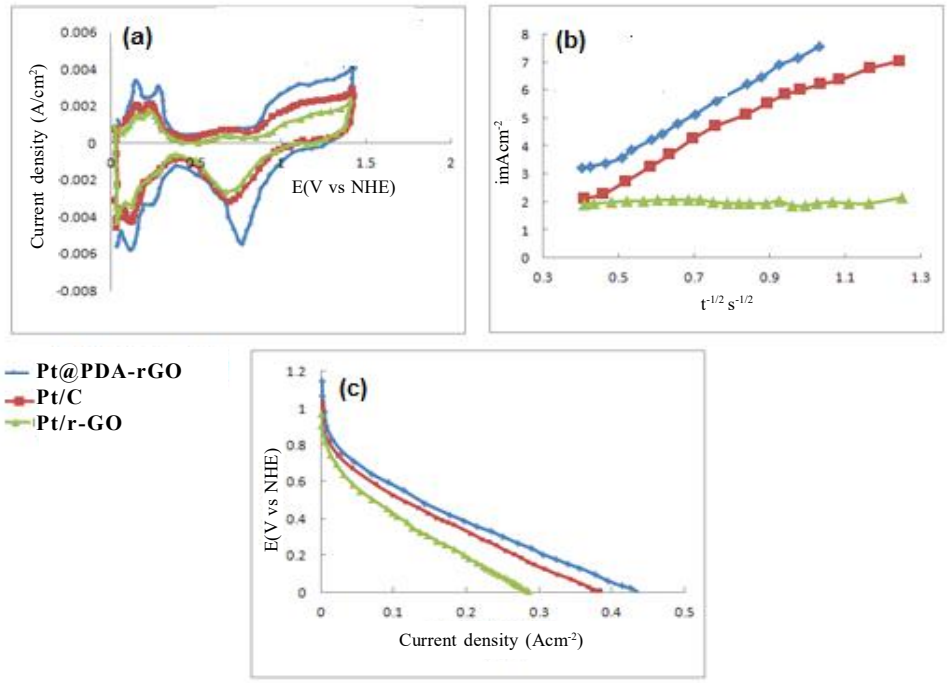

Fig. 6. (a) Cyclic voltammetry curves for the Pt@PDA-rGO, Pt/rGO and Pt/C (Electrochem) electrocatalysts for a scan rate of 50 mV s^{-1} at 25 ºC in 0.5M H_2SO_4 and N_2atomosphere .(b) Plots of I vs. $t^{-1/2}$ for oxygen reduction reaction.(c) Linear scan voltammograms of the Pt@PDA-rGO, Pt/rGO and Pt/C (Electrochem) for a scan rate of 1mV s^{-1} at 25 ºC in 0.5M H_2SO_4 and saturated oxygen atmospheres.

results are listed in Table 1 these results indicated that the permeability of oxygen in the Pt@PDA-rGO electrocatalyst is slightly higher than that of the Pt/rGo and Pt/C electrocatalyst,

Suggesting that the permeability of O_2 on the PDA-rGO is more favored than that on rGO and carbon black surface and this is in substantial agreement with the results of specific ECSA.

The electrocatalytic activity of Pt@PDA-rGO were compared to Pt/rGo and Pt/C (Electrochem) catalysts toward the electrochemical reduction of oxygen in the O2-saturated 0.5M H_2SO_4 at a scan rate of 1.0 mV s^{-1} in the potential range of 1.2 to –0.

3 V versus the Ag/AgCl reference electrode. The polarization curves for the electrodes in conventional three-electrode cells are presented in Fig. 6c. The ORR onset potentials for the Pt@PDA-rGO, Pt/rGo and Pt/C (Electrochem) are 1.142, 1.061 and 0.969 Vversus NHE, respectively. It should be noted that the open circuit potential of the Pt@PDA-rGO electrocatalysts in O_2 saturated solution is somewhat higher than that of the Pt/rGo and and Pt/C (Electrochem) proposing that the oxygen adsorption on the Pt@PDA-rGO surface is more preferred than that on pure Pt/C (Electrochem) and Pt/rGo surface .From the figure it can be easily seen that the kinetic current density of Pt@PDA-rGO is far larger than that of the Pt/C catalyst in the potential region 0.8 vs NHE.

The electrochemical kinetics parameters were obtained using the Tafel equation [36]:

$$\eta = \frac{2.303RT}{\alpha nF}\log\left(\frac{i}{i_0}\right) \quad (4)$$

Where η is the over potential, R the gas constant, T the absolute temperature, a the transfer coefficient, i0 the exchange current density, n the number of electrons, and F is the Faraday's constant. All current densities in Eq. (4) were calculated relative to the real area of the working electrode. In all polarization curves, two linear regions are observed in the Tafel plot for the ORR on Pt@PDA-rGO, Pt/rGO and Pt/C (Electrochem) electrocatalysts, the high current density regime (HCD) yields a slope of approximately 100-120 mV $decade^{-1}$. However, at low current densities (LCD) a clear linear region is observed with

Table 1: Tafel slope and exchange current density, Onset potential, ECSA

GDE	Exchange current Density (Acm^{-2})		Tafel slope ($mVdec^{-1}$)		Onset potential (V)	ECSA m^2g_{Pt}	Oxygen diffusion coefficient D_bc_b ($mol^{-1}\ cm^{-1}s^{-1}$)
Pt@PDA-rGO	LCD	5.51×10^{-5}	LCD	62	1.142	91.614	3.561×10^{-8}
	HCD	3.196×10^{-3}	HCD	123			
Pt/rGO	LCD	4.81×10^{-5}	LCD	67	1.061	85.712	3.172×10^{-8}
	HCD	2.155×10^{-3}	HCD	108			
Pt/C(Electrochem)	LCD	3.950×10^{-5}	LCD	72	0.969	80.212	2.422×10^{-8}
	HCD	1.819×10^{-3}	HCD	121			

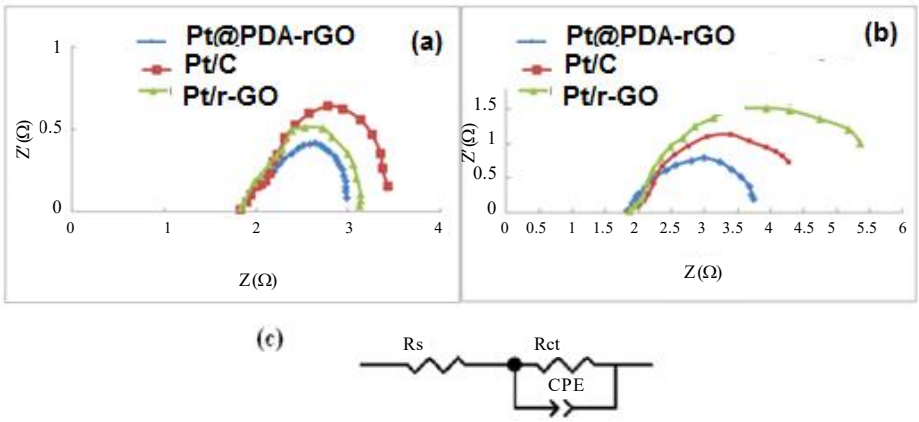

Fig. 7. EIS Nyquist plots in (a) 0.5 V and (b) 0.7 Vvs. NHE at 25 ºC in 0.5M H_2SO_4 and saturated oxygen atmospheres

a slope of 60-70mV decade^{-1}The obtained electrochemical parameters are seen in Table 1. The increased onset potential, exchange current density exhibited by Pt@PDA-rGO hybrid could be attributed to the changes in morphology to simplify fast reaction kinetics, and improve O_2molecular diffusion on the Pt surface. Furthermore, Pt nanoparticles interact with both the catechol groups of PDA and the graphitic plane.

The electron transfer kinetics of oxygen reduction in each electrode was studied by selected electrochemical impedance spectroscopy (EIS) measurements. Fig 6 shows representative Nyquist complex-plane impedance spectra of the electrodes) for ORR in 0.5 M H_2SO_4 at. 0.5 V and 0.7 V vs. NHE. Albeit the impedance spectra have analogous semicircular shapes, the diameters of the semicircle vary considerably As shown in Fig. 7(c), an electrochemical interface can be simulated by using a nonlinear regression with an equivalent electrical circuit $R_s(R_p$ CPE), where R_s is the sum of the electrode and electrolyte resistances, CPE is the double layer capacity, and R_{ct} is charge transfer resistance [37] The CPE (constant-phase elements represents the double-layer capacitance distributed between the ohmic and faradic processes. The obtained parameters are listed in Table 2. According to the results of charge transfer resistance (R_{ct}) in LCD (0.7 V) and HCD (0.5 V), we get the best result for Pt@PDA-rGO electrocatalyst. This result is in consistent with the values obtained for ECSA, exchange current density and the permeability of oxygen.

Long-term stability and durability of ORR catalysts is a serious commitment for fuel cell system. We carried out accelerated durability tests (ADT) by applying cyclic potential sweeps between 0.02 and 1.4 V vs NHE at 50 mV s^{-1} in N_2 purged 0.5 M H_2SO_4. Fig. 8 shows the 1 and1400th CV cycles for the Pt@PDA-rGO hybrid, from which a small degradation in performance is observed. For a clear understanding of CV durability, the normalized ECSA was plotted as a function of cycle number Fig. 8(d). The Pt/rGO (decreased by ~31% of the initial ECSA) and Pt/C (decreased by ~ 55% of the initial ECSA) catalysts

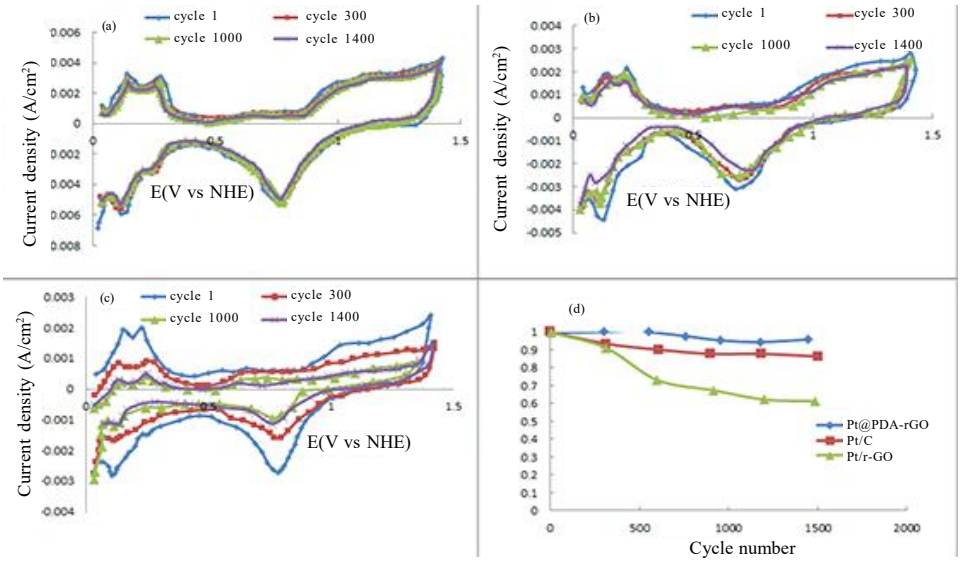

Fig. 8 .CV curves of 1, 300, 1000, and 1400 cycles for (a,b)Pt@PDA-rGO Pt/rGOand (c) Pt/C (Electrochem). (d) Comparison of ECSA loss for different materials.$ECSA_0$ is initial ECSA of corresponding catalys

Table2 Parameters obtained from EIS spectra with the equivalent circuit shown in Fig.6 using nonlinear least-squares fitting (Zview,ver.2.0)

Electrocatalyst	R_{ct} (Ω) at E=0.5 Vvs NHE	R_{ct} (Ω) at E=0.7 vs V vs NHE
Pt@PDA-rGO	1.021	1.921
Pt/rGO	1.292	2.442
Pt/C	1.611	3.523

presented an enormous loss in ECSA over 1400 cycles. In sharp contrast, a decrease in ECSA (<10%) is detected for the hybrid Pt@PDA-rGO. High concentrations of catechol and amine functional groups leads to strong interaction between support and metal which are few influenced by the acids and bases, moreover are safe to a certain extent over the electrostatic environmental changes under proton exchanges, which results in corrosion protection; otherwise, the Pt nanoparticles could aggregate together which could result in degradation of the catalytic activity. Furthermore hybrid structure, the flexible 2D profile of PDA-rGO may acts as a mesh that avoids leaching of dissolved Pt species into the electrolyte.

CONCLUSION

Briefly in this study, a simple but very efficient synthesis strategy has been developed for high loading of Pt on Graphenes, Well-dispersed Pt nanoparticles with small particle size were obtained on PDA-functionalized Graphene Pt@PDA-rGO. Through the noncovalent surface functionalization by PDA, large quantities of homogeneously distributed active sites can be produced for attaching Pt species. Compared to industrially adopted catalysts (i.e., state-of-the-art Pt/C catalyst the as-synthesized Pt@PDA-rGO and Pt/rGO hybrid shows an outstanding catalytic activity toward ORR, with respect to onset potential, exchange current density ,charge transfer resistance , the permeability and, stability, The effectively superior the electrocatalytic activity of Pt@PDA-rGO was ascribed to the follows: 1. The presence of PDA on the Graphene sheets could help the formation of small, highly concentrated and uniformly dispersed Pt nanoparticles at high Pt-loadings; 2. The PDA dispersed on Graphene sheets can increase the Graphene conductivity and the

rapidly removal of intermediate poisoning species; 3. The PDA can also prevent the aggregation of nanosheets, therefore, Pt nanoparticles can be loaded on both sides of Graphene, which can further reduce the aggregation of the nanosheets to produce much more nanoparticle dispersion and utilization on its surface Given that the ORR catalytic activity has been the rate-determining step in electrochemical energy devices, all those particular properties make us consider that Pt@PDA-rGO and Pt/rGO hybrid can be employed in next generation electrochemical energy devices.

CONFLICT OF INTEREST

The authors declare that there are no conflicts of interest regarding the publication of this manuscript.

REFERENCES

1. Viva, F. A.; Bruno, M. M.; Franceschini, E. A., et al. Mesoporous carbon as Pt support for PEM fuel cell, *International Journal of Hydrogen Energy*. 2014.
2. Tiwari, J. N.; Kemp, K. C.; Nath, K.; Tiwari, R. N.; Nam, H. G.; Kim, K. S. Interconnected Pt-nanodendrite/DNA/reduced-graphene-oxide hybrid showing remarkable oxygen reduction activity and stability, *ACS Nano*. 2013, *7,* 9223-9231.
3. Yuan XZ, W. H. *PEM fuel cell electrocatalysts and catalyst layers: fundamentals and applications*, Verlag London Ltd: Springer, 2008.
4. Wolf Vielstich , H. A. G., Harumi Yokokawa *Handbook of Fuel Cells: Advances in Electrocatalysis, Materials, Diagnostics and Durability, Volumes 5 & 6*: wiley, 2009.
5. Fournier, J.; Faubert, G.; Tilquin, J. Y.; Côté, R.; Guay, D.; Dodelet, J. P. High-performance, low Pt content catalysts for the electroreduction of oxygen in polymer-electrolyte fuel cells, *Journal of the Electrochemical Society*. 1997, *144,* 145-154.
6. Marinkas, A.; Arena, F.; Mitzel, J., et al. Graphene as catalyst support: The influences of carbon additives and catalyst preparation methods on the performance of PEM fuel cells, *Carbon*. 2013, *58,* 139-150.
7. Cong, H. P.; Wang, P.; Gong, M.; Yu, S. H. Facile synthesis of mesoporous nitrogen-doped graphene: An efficient methanol-tolerant cathodic catalyst for oxygen reduction reaction, *Nano Energy*. 2014, *3,* 55-63.
8. Allen, M. J.; Tung, V. C.; Kaner, R. B. Honeycomb carbon: A review of graphene, *Chemical Reviews*. 2010, *110,* 132-145.
9. Blanita, G.; Lazar, M. D. Review of graphene-supported metal nanoparticles as new and efficient heterogeneous catalysts, *Micro and Nanosystems*. 2013, *5,* 138-146.
10. Yoo, E.; Okata, T.; Akita, T.; Kohyama, M.; Nakamura, J.; Honma, I. Enhanced electrocatalytic activity of Pt subnanoclusters on graphene nanosheet surface, *Nano Letters*. 2009, *9,* 2255-2259.
11. Ji, K.; Chang, G.; Oyama, M.; Shang, X.; Liu, X.; He, Y. Efficient and clean synthesis of graphene supported platinum nanoclusters and its application in direct methanol fuel cell, *Electrochimica Acta*. 2012, *85,* 84-89.
12. Seger, B.; Kamat, P. V. Electrocatalytically active graphene-platinum nanocomposites. role of 2-D carbon support in pem fuel cells, *Journal of Physical Chemistry C*. 2009, *113,* 7990-7995.
13. Guo, S.; Zhang, S.; Sun, S. Tuning nanoparticle catalysis for the oxygen reduction reaction, *Angewandte Chemie - International Edition*. 2013, *52,* 8526-8544.
14. Chua, C. K.; Pumera, M. Selective removal of hydroxyl groups from graphene oxide, *Chemistry - A European Journal*. 2013, *19,* 2005-2011.
15. Stankovich, S.; Dikin, D. A.; Dommett, G. H. B., et al. Graphene-based composite materials, *Nature*. 2006, *442,* 282-286.
16. Mattevi, C.; Eda, G.; Agnoli, S., et al. Evolution of electrical, chemical, and structural properties of transparent and conducting chemically derived craphene thin films, *Adv Funct Mater*. 2009, *19,* 2577-2583.
17. Buzaglo, M.; Shtein, M.; Kober, S.; Lovrinèiæ, R.; Vilan, A.; Regev, O. Critical parameters in exfoliating graphite into graphene, *Physical Chemistry Chemical Physics*. 2013, *15,* 4428-4435.
18. Qu, K.; Wu, L.; Ren, J.; Qu, X. Natural DNA-modified graphene/Pd nanoparticles as highly active catalyst for formic acid electro-oxidation and for the Suzuki reaction, *ACS Applied Materials and Interfaces*. 2012, *4,* 5001-5009.
19. Zhang, M.; Xie, J.; Sun, Q.; Yan, Z.; Chen, M.; Jing, J. Enhanced electrocatalytic activity of high Pt-loadings on surface functionalized graphene nanosheets for methanol oxidation, *International Journal of Hydrogen Energy*. 2013, *38,* 16402-16409.
20. Xu, L. Q.; Yang, W. J.; Neoh, K. G.; Kang, E. T.; Fu, G. D. Dopamine-induced reduction and functionalization of graphene oxide nanosheets, *Macromolecules*. 2010, *43,* 8336-8339.
21. Hu, X.; Qi, R.; Zhu, J., et al. Preparation and properties of dopamine reduced graphene oxide and its composites of epoxy, *Journal of Applied Polymer Science*. 2014, *131*.
22. Lee, W.; Lee, J. U.; Jung, B. M., et al. Simultaneous enhancement of mechanical, electrical and thermal properties of graphene oxide paper by embedding dopamine, *Carbon*. 2013, *65,* 296-304.
23. Huang, Y.; Liu, Y.; Yang, Z., et al. Synthesis of yolk/shell Fe3O4-polydopamine-graphene- Pt nanocomposite with high electrocatalytic activity for fuel cells, *Journal of Power Sources*. 2014, *246,* 868-875.
24. Tian, J.; Deng, S. Y.; Li, D. L., et al. Bioinspired polydopamine as the scaffold for the active AuNPs anchoring and the chemical simultaneously reduced graphene oxide: Characterization and the enhanced biosensing application, *Biosensors and Bioelectronics*. 2013, *49,* 466-471.
25. Zhang, Q. L.; Xu, T. Q.; Wei, J.; Chen, J. R.; Wang, A. J.; Feng, J. J. Facile synthesis of uniform Pt nanoparticles on polydopamine-reduced graphene oxide and their electrochemical sensing, *Electrochimica Acta*. 2013, *112,* 127-132.
26. Zhou, H.; Liu, Y.; Chi, W.; Yu, C.; Yu, Y. Preparation and antibacterial properties of Ag@polydopamine/graphene oxide sheet nanocomposite, *Applied Surface Science*. 2013, *282,* 181-185.
27. Hummers Jr, W. S.; Offeman, R. E. Preparation of graphitic oxide, *Journal of the American Chemical Society*. 1958, *80,* 1339.
28. Shin, H. J.; Kim, K. K.; Benayad, A., et al. Efficient reduction of graphite oxide by sodium borohydride and its effect on electrical conductance, *Advanced Functional Materials*. 2009, *19,* 1987-1992.

29. Kheirmand, M.; Gharibi, H.; Abdullah Mirzaie, R.; Faraji, M.; Zhiani, M. Study of the synergism effect of a binary carbon system in the nanostructure of the gas diffusion electrode (GDE) of a proton exchange membrane fuel cell, *Journal of Power Sources*. 2007, *169,* 327-333.
30. Gharibi, H.; Faraji, M.; Kheirmand, M. The Role of PANI/Nafion on the Performance of ORR in Gas Diffusion Electrodes of PEM Fuel Cell, *Electroanalysis*. 2012, *24,* 2354-2364.
31. Ferrari, A. C.; Meyer, J. C.; Scardaci, V., et al. Raman spectrum of graphene and graphene layers, *Physical Review Letters*. 2006, *97*.
32. Antolini, E.; Giorgi, L.; Cardellini, F.; Passalacqua, E. Physical and morphological characteristics and electrochemical behaviour in PEM fuel cells of PtRu/C catalysts, *Journal of Solid State Electrochemistry*. 2001, *5,* 131-140.
33. Vidakoviæ, T.; Christov, M.; Sundmacher, K. A method for rough estimation of the catalyst surface area in a fuel cell, *Journal of Applied Electrochemistry*. 2009, *39,* 213-225.
34. Pozio, A.; De Francesco, M.; Cemmi, A.; Cardellini, F.; Giorgi, L. Comparison of high surface Pt/C catalysts by cyclic voltammetry, *Journal of Power Sources*. 2002, *105,* 13-19.
35. Allen J. Bard , L. R. F. *Electrochemical Methods: Fundamentals and Applications* Wiley, 2000 |.
36. Gharibi, H.; Javaheri, M.; Mirzaie, R. A. The synergy between multi-wall carbon nanotubes and Vulcan XC72R in microporous layers, *International Journal of Hydrogen Energy*. 2010, *35,* 9241-9251.
37. Yuan, X.-Z., Song, C., Wang, H., Zhang, J. *Electrochemical Impedance Spectroscopy in PEM Fuel Cells,Fundamentals and Applications*: Springer, 2010.